

## ■ Electro, Physical &amp; Theoretical Chemistry

## XAS Diagnostic of the Photoactive State in Co(II) Azobenzene Complex in Organic Solvents

Valery G. Vlasenko,<sup>\*,[a]</sup> Svetlana O. Shapovalova,<sup>[b]</sup> Alexander A. Guda,<sup>\*,[b]</sup> Anatolii V. Chernyshev,<sup>[c]</sup> Andrey G. Starikov,<sup>[c]</sup> Grigory Yu. Smolentsev,<sup>[d]</sup> Anatolii S. Burlov,<sup>[c]</sup> Sergey A. Mashchenko,<sup>[c]</sup> and Alexander V. Soldatov<sup>[b]</sup>

X-ray absorption spectroscopy (XAS) was used to characterize the structure of the photoactive Co(II) azobenzene complex. Optical absorption spectra show that photoinduced changes occur only in dimethylformamide (DMF) solvent, while in acetonitrile, this complex is photochemically inactive. Co K-edge XAS spectra indicate 6-coordinated species in acetonitrile with a structure similar to one in the crystalline form of the

complex. However, in DMF, an activation process occurs related to the decrease of coordination number, bond shortening and absorption edge shift to the higher energies. Quantitative analysis indicates that observed spectral changes are related to the high spin - low spin transition in the Co complex accompanied by the bond dissociation and solvent coordination.

## Introduction

Magnetic bistable coordination compounds are a suitable basis for creating high-capacity nonvolatile molecular memory, molecular switches, pressure sensors, contrast agents for magnetic resonance imaging.<sup>[1]</sup> The most common effect leading to the switching of the magnetic states of transition metal complexes is the spin-crossover (SCO), which consists in thermally initiated spin transitions in the inner electron shell of a metal.<sup>[2]</sup> A ligand-driven light-induced spin change (LD LISC), which was first detected in the Fe(II) styrylpyridine complexes,<sup>[3]</sup> appears promising. It is based on the photo-induced isomerization of the styrylpyridine ligand, which leads to a change in the strength of the ligand field. Recently, another promising approach has been proposed to control the magnetic properties of transition metal complexes, determined by the light-induced rearrangement of the ligand, which leads to a change in the coordination environment of the metal, and, as a consequence, its spin state, LD- CISSS (Light-Driven Coordination-Induced Spin-State Switching).<sup>[4]</sup> Like the above mentioned LD LISC,<sup>[3]</sup> it is caused by *cis-trans* isomerization of the ligand and is realized at room temperatures. In the present work, the

tion-Induced Spin-State Switching).<sup>[4]</sup> Like the above mentioned LD LISC,<sup>[3]</sup> it is caused by *cis-trans* isomerization of the ligand and is realized at room temperatures. In the present work, the

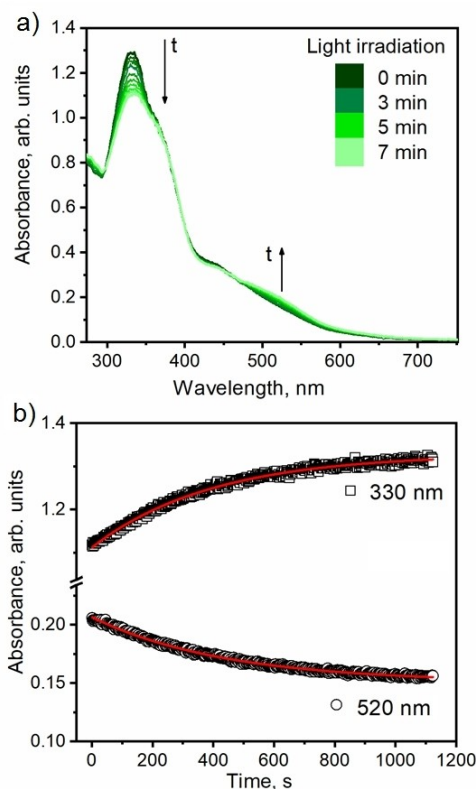


**Figure 1.** a) The changes in absorption spectra for I in DMF ( $C = 2.15 \cdot 10^{-5}$  M) upon irradiation ( $P = 12$  mW) by  $\lambda = 436$  nm at  $T = 293$  K. b) Absorbance changes for complex I at 330 nm and 520 nm, recorded during thermal relaxation after 365 nm irradiation. The red line is a monoexponential fit with a time constant  $\tau = 415$  s.

[a] Dr. V. G. Vlasenko  
Southern Federal University  
Institute of Physics  
Stachki ave. 194, 344090, Rostov-on-Don, Russian Federation  
E-mail: v\_vlasenko@rambler.ru

[b] S. O. Shapovalova, Dr. A. A. Guda, Prof. A. V. Soldatov  
Southern Federal University  
The Smart Materials Research Institute  
Sladkova street 178/24 A., Rostov-on-Don 344090, Russian Federation  
E-mail: guda@sfedu.ru

[c] Dr. A. V. Chernyshev, Dr. A. G. Starikov, Dr. A. S. Burlov, Dr. S. A. Mashchenko  
Southern Federal University  
Institute of Physical and Organic Chemistry  
Stachki ave. 194/2, 344090, Rostov-on-Don, Russian Federation

[d] Dr. G. Y. Smolentsev  
Paul Scherrer Institute  
Forschungsstrasse 111, 5232 Villigen, PSI, Switzerland

Supporting information for this article is available on the WWW under <https://doi.org/10.1002/slct.202101345>

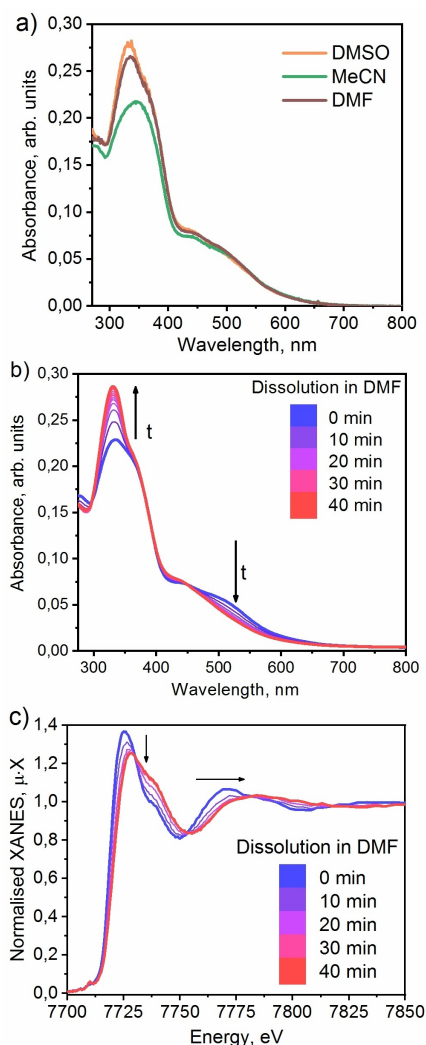


**Figure 2.** a) UV-Vis absorption spectra for complex I in different solvents after 1 hour of equilibration. b) Changes in the UV-vis absorption spectrum of the complex I in the DMF starting from the moment of dissolution. c) Changes in the Co K-edge XANES spectra of the complex I in DMF just after dissolution.

optical properties of bis[1-phenyl-3-methyl-4-[4-methyl-2-(4-methylphenylazo)-phenylamino-methylene]pyrazol-5-onate]cobalt(II) (I) containing a photochemically active azobenzene

group are studied (Scheme 1, see Supplementary Material for synthetic and analytical details). The increased interest in this complex is due to its structure. In accordance with the results of single-crystal XRD,<sup>[5]</sup> the used ambidentate ligands occupy three crystallographic sites near the central metal atom, unlike bidentate ligands in previously studied complex bis[1-phenyl-3-methyl-4-[4-methyl-2-(4-methyl-phenylazo)phenylamino-methylene]pyrazol-5-onate]cobalt(II) (II) containing an azo group in the *para*- positions of the amine fragment of ligand<sup>[5]</sup> (Scheme 1). The elongated bonds between the cobalt ion and the nitrogen atoms of the azobenzene groups (2.2510(14) Å, 2.2889(15) Å) indicate the possibility of their dissociation as a result of light irradiation.

However, different behaviour of the complex was observed in DMF and acetonitrile solutions. In the former case, UV-vis studies revealed photoinduced changes while in the acetonitrile, the complex was photoinactive. This study aims to analyze the local atomic and electronic structure of the Co complex after its dissolution to address its photochemical behavior. The first step in understanding which of these mechanisms is realized for given material is to understand the structure of complex in the photoactive form, which can be significantly different from the crystal structure of initial material.

## Results and Discussion

UV-Vis absorption spectrum of Co(II) complex I (figure 1a) shows two absorption bands. Intense short wavelength ( $\epsilon = 43500 \text{ M}^{-1}\text{cm}^{-1}$ ) band in the 300–400 nm region with a maximum at 346 nm is due to  $\pi\text{-}\pi^*$  transitions. Diffuse band in the region of 400–600 nm has a weak maximum at 442 nm ( $\epsilon = 14800 \text{ M}^{-1}\text{cm}^{-1}$ ) and a shoulder at 508 nm ( $\epsilon = 10400 \text{ M}^{-1}\text{cm}^{-1}$ ) which can be assigned to an intramolecular charge transfer  $n \rightarrow \pi^*$  transition of azo-aromatic chromophore.<sup>[6]</sup> This absorption is attributed to the existence of azo-imine and azo-enamine tautomeric transformations of the azo-ligands on highly polar solvents.<sup>[7]</sup> Two main absorption bands change their intensity as indicated by arrows in figure 1a in DMF solution. Both 436 nm and 365 nm UV light irradiation induced similar absorption spectra changes, resulting in a decrease of intensity of 330 nm band and a slight increase of 530 nm band's intensity.

**Table 1.** Bond distances R (Å) from DFT calculations for the Co(II) complexes I and from EXAFS-analysis (fixed factor Debye-Waller  $\sigma^2 = 0.0033 \text{ Å}^2$ , R-factor below 5%).

Distances R, Å	DFT									EXAFS powder	DMF equilibrated
	la	lb	lc	ld	le	lf	lg	lh	li		
Co–N1	2.08	1.94	2.06	1.95	2.03	2.10	2.26	1.99	2.23	2.06	1.95
Co–N2	2.08	1.94	2.08	1.99	2.03	2.14	2.11	2.03	2.17	2.06	1.95
Co–N3	2.36	2.23	2.32	2.05	–	–	–	–	–	2.24	–
Co–N4	2.36	2.23	–	–	–	–	–	–	–	2.28	–
Co–O1	2.11	2.12	2.12	1.97	1.97	2.14	2.00	2.14	2.10	2.06	1.90
Co–O2	2.11	2.12	2.01	2.11	1.97	2.05	2.01	1.94	2.10	2.06	1.90
Co–solv	–	–	–	–	–	2.18	2.16	2.03	2.24	–	2.06
Co–solv	–	–	–	–	–	–	–	–	2.19	–	–
Average	2.18	2.10	2.12	2.01	2.00	2.12	2.11	2.03	2.17	2.13	1.95

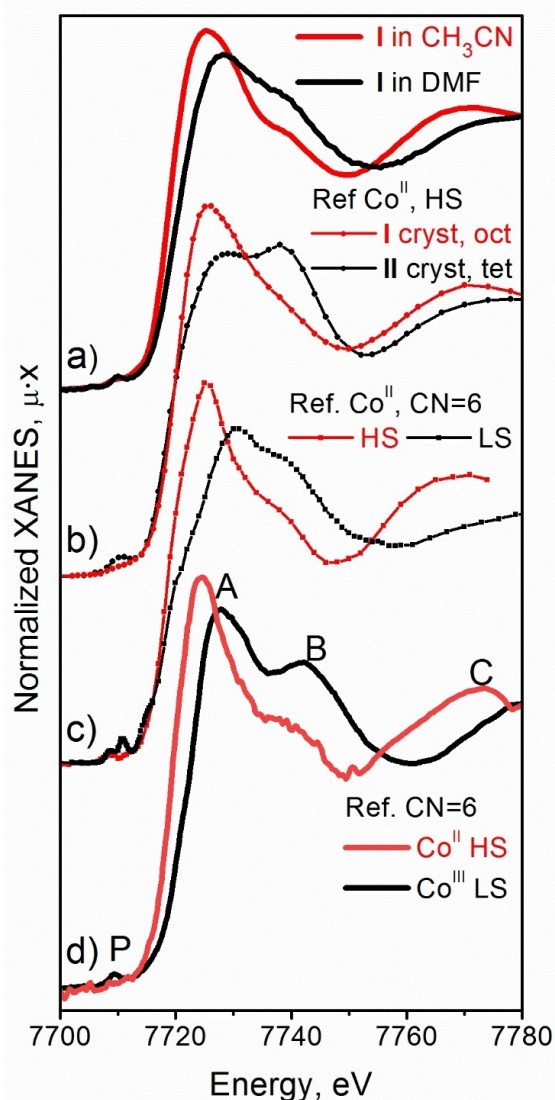
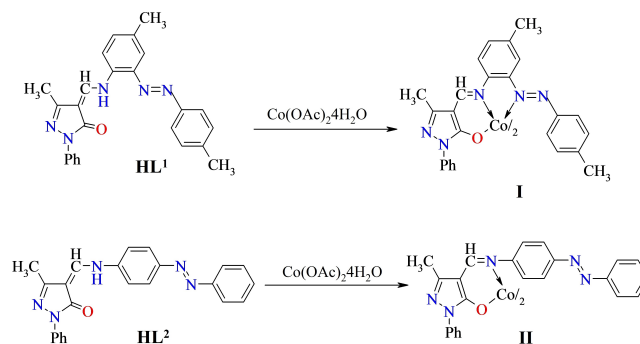


**Figure 3.** Co K-edge XAS measured for the: a) complex I in acetonitrile and DMF solvents, b) crystalline powder of two high spin Co(II) complexes – 6-coordinated complex I and 4-coordinated complex II, c) reference 6-coordinated Co(II) structures revealing only spin transition, the high spin Co(apy)<sub>2</sub>Br<sub>2</sub> and the low spin cobaloxime,<sup>[10]</sup> d) reference structures of the valence tautomer 6-coordinated Co complex<sup>[11]</sup> revealing both spin and charge transition.

The observed photoinitiated changes in the spectra are characteristic of the azobenzenes E/Z-isomerization<sup>[8]</sup> and can be attributed to the photoreaction of the E/Z-isomerization relative to the N=N double bond in the ligand. A thermal back-reaction occurs after a light is switched off. The kinetics of dark relaxation of the Z-isomer of the ligand of complex I (figure 1b) is described by a mono-exponential dependence, from which the lifetime  $\tau = 415$  s was obtained, which is comparable to the thermal relaxation times of azomethine complexes with E/Z-isomeric azo fragments not included in the coordination site.<sup>[9]</sup> The complex reveals photoinduced transformations only in the DMF and DMSO solutions but not in CH<sub>3</sub>CN (see Suppl.



**Scheme 1.** Synthesis of the high spin 6-coordinated Co complex I and 4-coordinate high spin analogue Co complex II.

Information). As shown in figure 2a, the UV-vis spectrum of I in acetonitrile was different from ones acquired in DMF and DMSO solvents. While being inactive upon irradiation the shape of the absorption spectrum in acetonitrile was similar to the photoaccumulated state in DMF.

Therefore, we conclude that the structure of the complex changes both upon light stimuli and the interaction with DMF solvent molecules. Figures 2b and 2c highlight the dynamics of the structural changes upon dissolution in DMF.

Immediately after the dissolution, the UV-vis absorption spectrum of the complex in CH<sub>3</sub>CN and DMF are similar. However, within the first hour, a transformation of the spectrum occurs in DMF, consisting in an increase of the band in the region of 300–400 nm and a decrease in the long-wavelength shoulder intensity at  $\lambda > 450$  nm (figure 2b). Interestingly that these changes are similar to ones observed upon irradiation. The clear isobestic points indicate the presence at each time only two forms of compounds in the solution that absorb in this spectral region.

After dissolution in DMF and acetonitrile, Co K-edge XANES indicated pseudo-octahedral coordination of Co(II) complex I with distances analogous to the crystalline phase (see Table 1 and Suppl. Information for the details of EXAFS analysis). The subsequent behaviour of solutions in DMF and acetonitrile is different. The Co K-edge XANES does not change in the acetonitrile, indicating the absence of any bond dissociation or complex coordination by solvent molecules. In contrast, dissolution in DMF induces gradual changes in the complex spectra indicated by arrows in figure 2c. The number of spectra recorded in the series has isobestic points, indicating the transition between two states. The final state (blue experimental spectrum) has a lower intensity of peak A, and the higher intensity of peak B and peak C shifted to higher energies. This tendency is similar to the changes between octahedral and tetrahedral Co(II) species,<sup>[5]</sup> indicating a decrease of the cobalt coordination number in DMF.

To further investigate the crystalline Co complex I structure and solvated forms in DMF and acetonitrile, we measured a series of reference samples characterized by different Co valence, spin state and coordination number. Pair (b) of spectra in figure 3 shows Co K-edge XAS measured for the crystalline

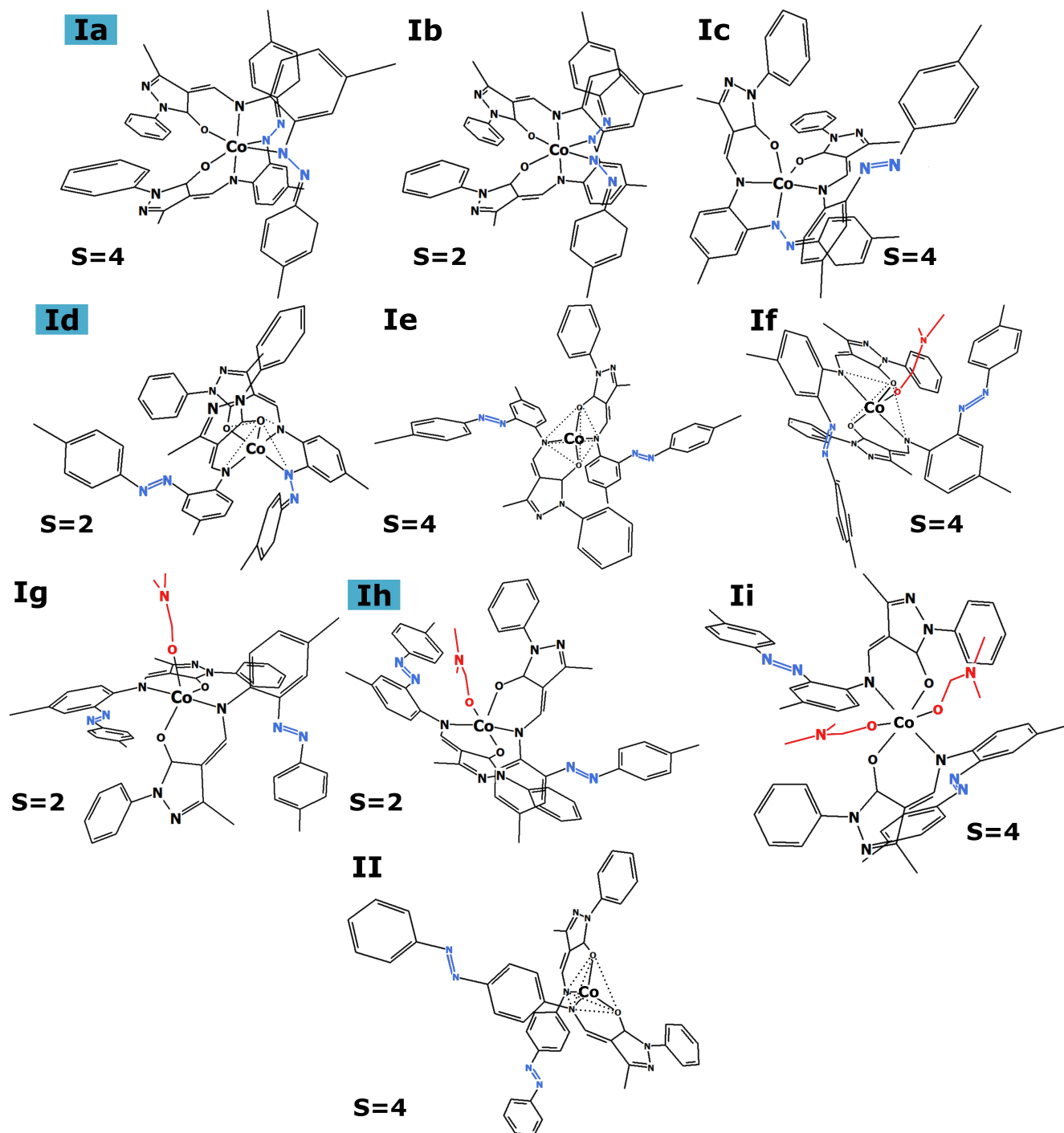
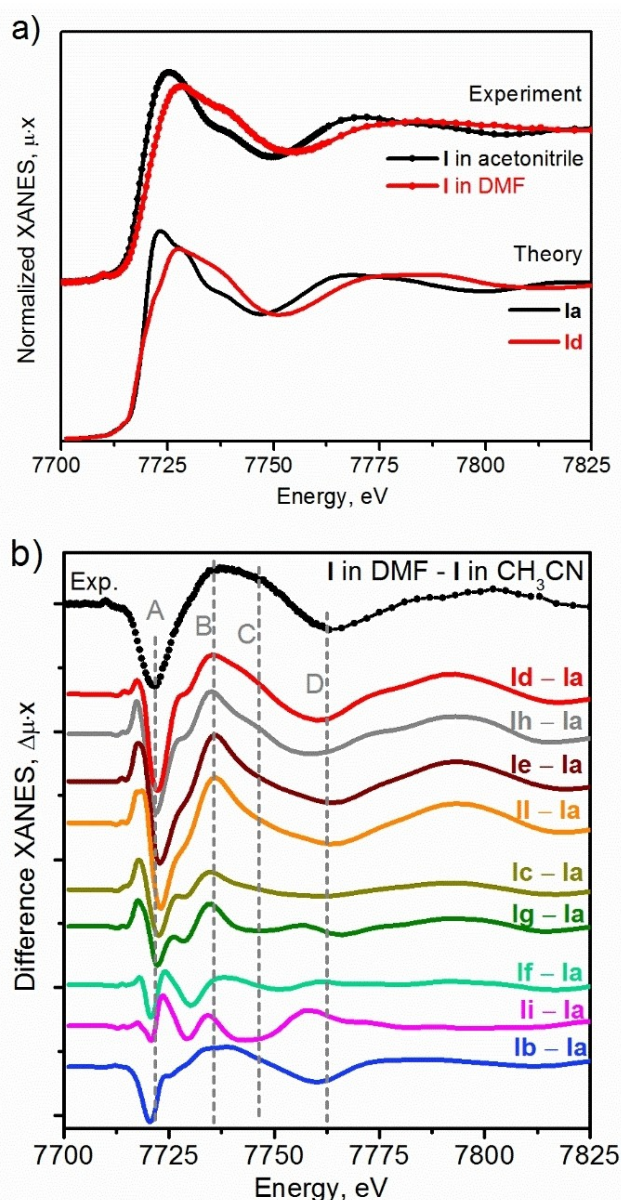


Figure 4. The DFT optimized structures of complex I with and without coordinating DMF molecules and complex II ( $S=4$  for HS,  $S=2$  for LS).

high spin (HS) Co(II) 6-coordinated (complex I) and 4-coordinated complex II - bis[1-phenyl-3-methyl-4-[4-methyl-2-(4-methyl-phenylazo)phenylaminomethylene]pyrazol-5-onate]cobalt(II) containing an azo group in *para*-positions of the amine fragment<sup>[5]</sup> (see Scheme 1). XANES spectrum for the tetrahedral complex II has a smaller intensity of peak A, stronger peak B intensity, and the peak C shifted to the higher energies. The pre-edge feature P around 7710 eV has a higher intensity for

the I in DMF and tetrahedral complex II due to larger 3d–4p mixing for noncentrosymmetric coordination.

For complexes with low symmetry distortions, for example, with the octahedral environment of cobalt ions, the pre-edge features P arise only from electric-quadrupole transitions. Their intensity is substantially lower than in the case of Co 4p–3d mixing. However, the pair of XANES spectra shown at Figure 3b does not fully describe the spectral changes observed in the



**Figure 5.** a) Experimental Co K-edge XAS measured for the complex I after dissolution in DMF and  $\text{CH}_3\text{CN}$  are compared to the theoretical calculations for the structures Ia and Id from figure 4. b) Difference between experimental spectra in panel a) is compared to the differences between theoretical spectra for structures Ia–Ii. The order of the curves is selected by decreasing their similarity from the experimental graph.

Figure 3a. The energy shift of the absorption edge between spectra in different solvents is larger than between 4- and 6-coordinated Co(II) complexes in the high spin state.

Pair (3c) of spectra in figure 3 shows the changes upon spin transition in pseudooctahedral Co(II) complexes. The Co center in the cobaloxime complex is coordinated by two solvent molecules at a larger Co–L distance compared to the four Co–N equatorial distances.<sup>[10]</sup> Spectral changes in pair (3c) reproduce both the energy shift and intensity variations of peaks A, B, C.

Finally, by using pair (3d) we exclude the change of the oxidation state in complex I upon dissolution in DMF. Indeed, the spectrum of 6-coordinated Co(III) in the low spin state after valence tautomer transition<sup>[11]</sup> is shifted by 3 eV from the high spin Co(II) state of the same complex. The same shift measured at half of the rising edge intensity for the spectra in acetonitrile and DMF equals only 1.7 eV.

To address the structural transition of the complex in DMF, we have performed DFT simulations for the set of models with and without coordinating solvent molecules. For each structure then the theoretical Co K-edge XANES spectrum was calculated and compared to the experimental data. Figure 4 shows the geometries after relaxation. According to XRD data, complex I is characterized by a pseudo-octahedral coordination unit. Photoactive fragment isomerization of one of the ligands leads to Ic structure, the central atom of which is pentacoordinated. The low-spin Id structure with such a coordination site is the least favourable isomer of complex I. Simultaneously, the Ie structure, which includes two bidentate bound ligands, is destabilized relative to the Ia ground state, which allows us to expect the presence of an isomer with a tetracoordinated central atom in the complex solutions.

The most preferred adduct form of complex I with one DMF molecule corresponds to the Ig structure, including two bidentate linked ligands and an axially coordinated solvent molecule. A slight destabilization of the If model, which has a distorted octahedron structure, indicates the possibility of the presence of both high-spin forms in the solution.

Figure 5a shows calculated spectra for the DFT optimized structures, which agree best with the experimental data. In figure 5b we compare the experimental difference spectrum with all theoretical differences calculated with respect to the spectrum of model Ia. Two structures, namely Id and Ih reproduce relative intensities of features A, B and C in the experimental data. The distances in Id and Ih are in good agreement with EXAFS analysis.

Dissolution of the complex in DMF will dissociate cobalt donor-acceptor bonds with nitrogen atoms of the azobenzene group. Being a coordinating solvent, DMF will try to fill vacancies in the inner coordination sphere of the metal. If both bonds were broken synchronously, an adduct with two axially coordinated DMF molecules would most likely be formed. However, such a mechanism is unlikely since it assumes preliminary photoinduced *cis-trans* isomerization. The most preferred route is in which one DMF molecule is “squeezed” to the central atom, which contributes to forming a coordination polyhedron (e.g. trigonal bipyramid) that blocks the approach of the second solvent molecule. All the energy differences predicted by the DFT method can be overcome under photochemical conditions.

## Conclusion

XAS spectroscopy was applied to the Co(II) complex with two photoactive azobenzene groups. The complex showed photo-induced UV-vis spectral changes upon 330 and 436 nm irradiation in DMF and DMSO solutions, while in  $\text{CH}_3\text{CN}$ , it was

photo inactive. The crystalline form of the complex has pseudo-octahedral coordination, which remained unchanged upon dissolution in acetonitrile. Immediately after dissolution in DMF pseudo-octahedral structure is also retained and then undergoes transition during the one hour. Only the final form of the material is photoactive. After EXAFS analysis and theoretical XAS simulations, we attribute observed changes to the reduce in coordination number from 6 to 5. The final state can be described by a mixture of low spin Co(II) isomers with possible DMF molecule coordination. Photo activity of the complex in DMF is attributed to the E–Z isomerization of the azobenzene group dissociated from the Co atom.

## Supporting Information Summary

Details of the experimental procedures, corresponding references and characterization data for the synthesized compounds are provided in supporting information.

## Acknowledgements

Measurements and spectra analysis were carried out within the framework of the project of the Russian Foundation for Basic Research (RFBR#18-02-40029). S.O. Shapovalova acknowledges her PhD support from Russian Foundation for Basic Research (RFBR#20-32-90046) for a travel opportunity.

## Conflict of Interest

The authors declare no conflict of interest.

**Keywords:** photoswitchable molecules · Co(II) complex · Azo compounds · spin transition · X-ray absorption spectroscopy

- [1] a) O. Kahn, C. J. Martinez, *Science* **1998**, *279*, 44–48; b) M. A. Halcrow in *Spin-Crossover Materials: Properties and Applications*, John Wiley & Sons: Chichester, **2013**, 564; c) V. I. Minkin, *Russ. Chem. Bull.* **2008**, *57*, 687–717; d) S. M. Aldoshin, A. I. Zenchuk, E. B. Fel'dman, M. A. Yurishchev, *Russ. Chem. Rev.* **2012**, *81*, 91–104; e) S. S. Simon, M. Duran, J. J. Dannenberg, *J. Chem. Phys.* **1996**, *105*, 11024–11031; f) J. Linares, E. Codjovi, Y. Garcia, *Sensors* **2012**, *12*, 4479–4492.
- [2] a) P. Gutlich, H. A. Goodwin, *Top. Curr. Chem.*, Springer, Berlin, **2004**, 233–235; b) L. Cambi, L. Zego, *Ber. Dtsch. Chem. Ges.* **1931**, *64*, 2591–2698; c) S. Decurtins, P. Gutlich, C. P. Kohler, H. Spiering, A. Hauser, *Chem. Phys. Lett.* **1984**, *105*, 1–4.
- [3] C. Roux, J. Zarembowitch, B. Gallois, T. Granier, R. Claude, *Inorg. Chem.* **1994**, *33*, 2273–2279.
- [4] a) S. Venkataramani, U. Jana, M. Dommaschk, F. D. Sonnichsen, F. Tuzcek, R. Herges, *Science* **2011**, *331*, 445–448; b) S. Thies, H. Sell, C. Bornholdt, C. Schutt, F. Kohler, F. Tuzcek, R. Herges, *Chem. Eur. J.* **2012**, *18*, 16358–16368.
- [5] A. S. Burlov, S. A. Mashchenko, V. G. Vlasenko, K. A. Lyssenko, A. S. Antsyshkina, G. G. Sadikov, V. S. Sergienko, Yu. V. Koshchenko, Ya. V. Zubavichus, A. I. Uraev, D. A. Garnovskii, E. V. Korshunova, S. I. Levchenkov, *Rus. J. Coord. Chem.* **2015**, *41*, 376–386.
- [6] a) M. Ghasemian, A. Kakanejadifard, F. Azarbani, A. Zabardasti, S. Kakanejadifard, *Spectrochim. Acta Part A* **2014**, *124*, 153–158; b) Z. Shaghaghghi, G. Dehghan, *Acta Chim. Slov.* **2018**, *65*, 670–678.
- [7] F. Sahan, M. Kose, C. Hepokur, D. Karakas, M. Kurtoglu, *Appl. Organomet. Chem.* **2019**, *33*, e4954.
- [8] E. R. Talaty, J. C. Fargo, *Chem. Commun.* **1967**, *2*, 65–66.
- [9] A. D. Garnovskii, A. S. Burlov, A. G. Starikov, A. V. Metelitsa, I. S. Vasil'chenko, S. O. Bezugliy, S. A. Nikolaevskii, I. G. Borodkina, V. I. Minkin, *Russ. J. Coord. Chem.* **2010**, *36*, 479–489.
- [10] G. Smolentsev, B. Cecconi, A. Guda, M. Chavarot-Kerlidou, J. A. van Bokhoven, M. Nachtegaal, V. Artero, *Chem. Eur. J.* **2015**, *21*, 15158–15162.
- [11] A. A. Guda, M. Chegerev, A. Starikov, V. G. Vlasenko, A. Zolotukhin, M. Bubnov, V. Cherkasov, V. Shapovalov, Y. Rusalev, A. Tereshchenko, A. Trigub, A. Chernyshev, A. Soldatov, *J. Phys. Condens. Matter* **2021**, *33*, 215405 (9pp). doi.org/10.1088/1361-648X/abe650.

Submitted: April 13, 2021

Accepted: July 15, 2021